

# Laser Assisted Diagnostics for Characterization of Condensed Phases during Diesel Combustion Processes

R. Ragucci

*Istituto di Ricerche sulla Combustione  
c/o Facoltà di Ingegneria*

*P.le Tecchio  
80125 Napoli  
Italy*

A. Cavaliere

*Università di Pisa*

A.D'Alessio  
*Università di Napoli*

## ABSTRACT

A two-dimensional laser light scattering technique is presented for the detection of the condensed phase characteristics in a diesel combustion process. The paper deals with general aspects of this type of diagnostics to give an introduction to the future user of the techniques.

Preliminarily the relevance of different length scales of the scatterers and of the discretized elements of the detectors as well as the correspondence between the object field and the image pattern is presented. Afterwards the meaning of the scattering characteristics is discussed and selected examples of the possible use of the technique in diesel-like environment are presented.

## INTRODUCTION

The condensed phases present in a diesel, namely the injected liquid fuel and the carbonaceous products, originated in the fuel-rich pyrolytic regions, can be considered the skeleton of the diesel combustion processes.

In fact a complete characterization of them allows to follow the initial stages of the combustion, i.e. atomization, dispersion, vaporization, liquid pyrolysis, as well as the stages of soot formation and oxidation. These types of characterization have been widely performed on stationary spray combustion exploiting laser light scattering effects with single-point time-averaged measurements /1/. In this paper an extension of these techniques is presented in relation to time-resolved measurements on two-dimensional patterns.

The emphasis is posed on technological and methodological aspects rather than on chemical and physical evolution of the diesel combustion process. Therefore the experimental results will be presented in order to evidence features, advantages and shortcomings of the technique quoting the papers where results are presented in the framework of the process analysis.

The guide-line of the paper follows the possible applications of a specific optical set-up presented in the next section. But the generalization to different optical schemes should be clearly evident also where it is not explicitly commented.

The role of the two-dimensional quantitati-

ve optical diagnostics deserves a preliminary comment. It can be considered the "minimum level" of diagnostics in the analysis of turbulent unsteady inhomogeneous fields, with "small" length scales (like diesel sprays) because it allows spatial correlations in single and/or multiple patterns. Other possibilities, like conditional averaging or temporal profiles of single point measurements, can be deceptive because they miss to evaluate the relevance of the sampling point in the whole field. For instance a slight shift of the spray cross section between two different injections and/or during one injection may infer that the fixed sampling volume can be crossed alternatively by the central part or the peripheral one of the spray. So that the ensemble of measurements refers to very different conditions and any kind of average smooths away the real inhomogeneity of the two-phase field.

It is a matter of fact that a complete description of a two phase, turbulent, reactive, unsteady field is obtained only by means of the detection of three dimensional patterns collected along the whole temporal evolution of the process. But this has to be considered the final achievement of the diagnostics techniques, even though the first measurements of multi-dimensional imaging "simple" aerodynamic pattern /2/ have been performed. This techniques consist in a consecutive collection of spatially shifted planar images. Therefore it seems that also for this future application the detection of two dimensional patterns is a crucial step and the analysis of the measure methodology as well as the result interpretation should be useful not only for the present user but also for new generations of imaging systems.

The last preliminary comment is addressed to the quantitative nature of the visualization techniques presented in the paper. In fact its main difference with traditional photography of emission, scattering or extinction patterns is the use of an illuminating source (laser) which crosses the control volume with known energy flux and of a detecting device (intensified CCD camera) with linear repeatable sensitivity which allows accurate measure of the photons originated from the control volume.

## OPTICAL AND DATA ELABORATION SET-UP

The basic scheme of a two-dimensional laser light scattering set-up that can be used for the characterization of an unsteady turbulent reacting flow, like an igniting diesel spray, is presented in Fig. 1.

It is characterized by few essential parameters: power and repetition rate of the light source, sensitivity, spatial resolution and dynamic range of the detector, numeric resolution of the A/D converter. Another important aspect is the versatility and time resolution of the time controlling unit.

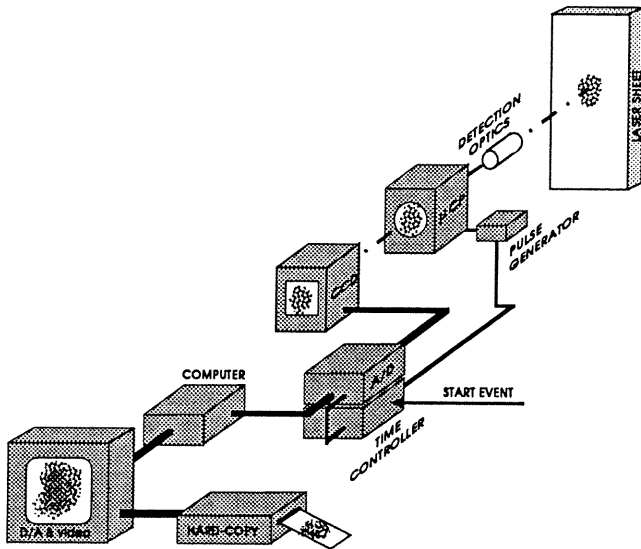


Fig.1 Optical set-up.

The light source used is a Nd-YAG laser whose pulse duration is 15 ns. The choice of this source has been suggested by the need of very short and strong illumination of the observed field. In fact the short pulse duration ensures a sufficient time resolution, while the high energy of light pulse allows to perform measurements also in case of experiments (like fluorescence applications) characterized by low light signals.

The laser beam is shaped as a thin collimated light sheet by means of a cylindrical telescope, which is constituted of two cylindrical confocal lenses. The light sheet is spatially filtered by means of a slit in order to select only the central part of the laser sheet with a nearly uniform intensity profile. The depth of the laser sheet is determined by a third cylindrical lens that focuses the sheet on the scattering volume. The depth of the laser sheet determine the depth of the probe volume. So that it can be convenient to have a very thin laser sheet in order to have higher spatial resolution.

The collecting optics focuses the illuminated field on the entrance section of an image intensifier. The numerical aperture of the collecting optics determines its depth of field and angle of acceptance that must be kept, in general, as small as possible.

The microchannel plate ( $\mu$ CP) image intensifier unit is used for two main tasks. In fact it allows either to detect low level light signal and to obtain time controlled exposing windows. The capability to detect also very low signals

(coupled with a high energy light source) allows to perform scattering measurements also in the less concentrated region of the spray and to perform fluorescence and emission measurements from the reacting regions of the spray. Furthermore it allows to use very high magnification ratios in order to obtain high spatial resolution.

The synchronization of the exposure with the laser pulse in scattering and fluorescence experiments allows to reject the luminous background from the ignited regions (in this case the temporal resolution comes from the very short time duration of laser pulse). The gateable characteristics of image intensifiers, on the other side, gives the possibility to perform time resolved measurements of emission from burning regions.

The light incident on the photocathode of  $\mu$ CP generates electrons that, if the  $\mu$ CP is energized, are accelerated by means of a venetian blind structure and of a bundle of optics fibres on a phosphorus screen. The choice of the photocathode and of phosphorus type affects the performances of the detecting system in terms of spectral responsivity and repetition rate.

The image obtained on the  $\mu$ CP output screen is collected by a solid state CCD camera. The sampled image are then digitized by means of an Analog to Digital converter. The number of detecting elements of  $\mu$ CP and CCD determine the spatial resolution of the whole system. In this case the limiting device is the  $\mu$ CP that presents the lower number of detecting elements (300x300). Anyway the digitalization of the images is performed on a finer numerical grid of 512x512 picture elements (pixels) in order to avoid moire phenomena occurrence. Concerning the dynamic range and accuracy limits of the detecting system it can be state that, providing that a good coupling of the various electronic components of the detecting system (that is a correspondence of the linear sensitivity ranges of intensifier and CCD camera) has been achieved, the dynamic range of the whole detecting system is determined by the component with the narrowest dynamic range (i.e. the intensifier). In correspondence of this dynamic range the resolution (i.e. the accuracy) of the measurements is fixed by the 8 bit digitalization of the analog to digital converter. Therefore, on decimal scale, integer numbers ranging from 1 to 256 (28) are representative digits and the accuracy is 1/256 of the saturation value.

## SINGLE IMAGE SYSTEMS

The scattering pattern collected by only one camera poses the fundamental problems of pattern recognition, common to any kind of visualization systems based on discretized detecting devices and on coherent illuminating sources.

The discretization of the sensitive area either for the microchannel plates and the CCD camera introduce as comparative length the size ( $l_p$ ) of a picture element (pixel) in the image plane. This length has to be compared with the characteristic dimension of the single scatterer  $l_s$  and of the average distance between the scatterers  $l_n$ .

In Fig.2 a schematic representation of the possible experimental conditions, which can

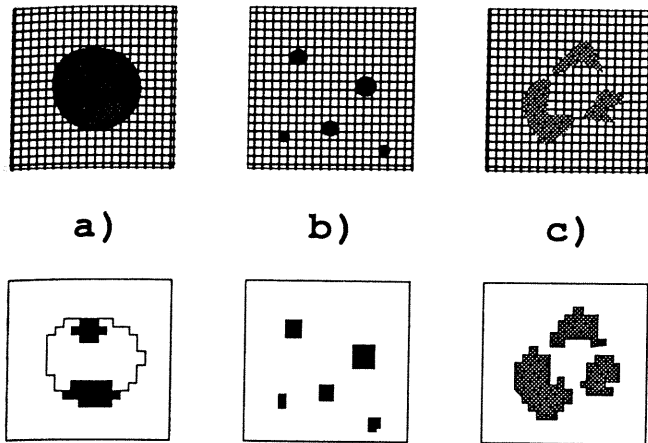


Fig. 2 Schematic representation of three possible experimental conditions, which can occur when different objects are imaged under different magnification

occur for different magnification ratios, is reported. In the case the particle is much larger than the pixel size ( $l_s \gg l_p$ ) the shape of the particle in the laser light scattered pattern is not the cross section of the particle because the collimation of the light on large particles entails an impact region of the light, which is scattered in narrow angular region. For instance in the lower part of Fig. 2a the scattered pattern collected at  $\theta=90^\circ$  for illumination from the bottom of a  $40 \mu\text{m}$  droplet, is reported. Two regions are clearly distinguishable; the lower one is due to the reflection and the higher one to the surface wave [1], which are generated from an impact region on the back side of the droplets. It is worthwhile to evidence, that in the case white-light uncollimated illumination is used the scattered pattern of the droplet is "filled" and the image shape resembles more the object shape. A complete discussion of this case can be found in the references [3]. In the case, sketched in Fig. 2b, the particles are comparable or smaller than the image pixel size ( $l_s \leq l_p$ ) and smaller than their distance ( $l_s < l_p$ ). In this case the scattered light (see lower part) is collected by one pixel or by few contiguous pixels. The image shape is not related to the particle shape and the only geometrical correspondence between object and image is the distance among the particles.

The third limit case, reported in Fig. 2c, refers to scatterers smaller than the image pixel ( $l_s < l_p$ ), whose mutual distances are smaller than the pixel size ( $l_n < l_p$ ). The image shape, reported in the lower part of Fig. 2c, is the discretized contour of the droplet cloud. A single connected region refers to an ensemble of droplets and the connectedness level (the number of single connected regions) is a measure of the droplets dispersion but it is not related to microscopic dispersion. Examples of these types of image are reported in reference [4]. The conclusion, relative to these laser light scattering images, is that morphological recognition is not possible in terms of particle size, but only in terms of distances among particles.

The scattered light intensity is distribu-

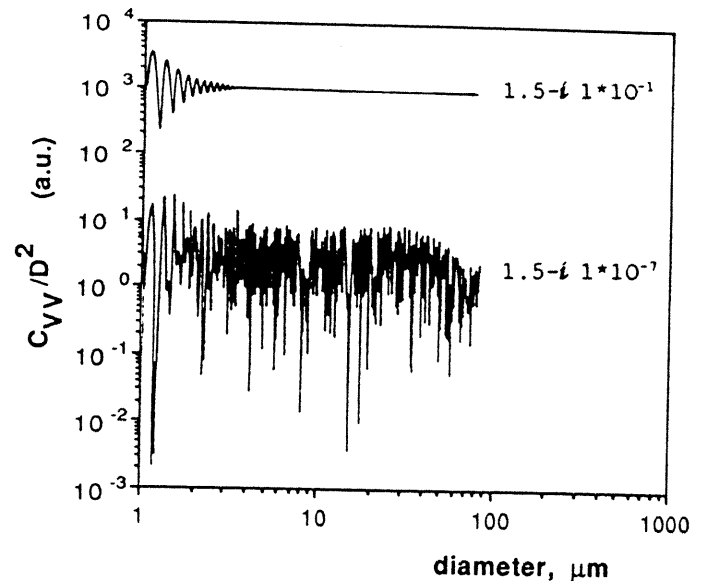


Fig. 3 Computed profiles of  $C_{vv}/D^2$  vs droplet size for two values of refractive index of  $1.5 \cdot 10^{-7}$  and  $1.5 \cdot 10^{-1}$  (displaced upward by a factor of  $10^8$ ).

ted according to dimension, shape and optical refractive index ( $m$ ) of the particles. This kind of dependence is shown in Fig. 3 in terms of  $C_{vv}/D^2$  vs droplet size  $D$ , reported for droplets (spheres) with  $m=1.5 \cdot 10^{-7}$  (a typical value for light oil fuels) and  $m=1.5 \cdot 10^{-4}$  (a value relative to a highly absorbing media) and for a scattering angle  $\theta=90^\circ$ . The vertically polarized cross section  $C_{vv}/5$ , computed by means of a numerical code [6] developed on the ground of Mie theory, is a measure of the scattering intensity for a single drop when it is multiplied for a constant dependent only on experimental conditions [5]. It is evident the oscillatory behaviour of the plot with an average dependence of  $C_{vv}$  on the square of droplet size. This is considered a drawback for size determination of single droplets due to the not single

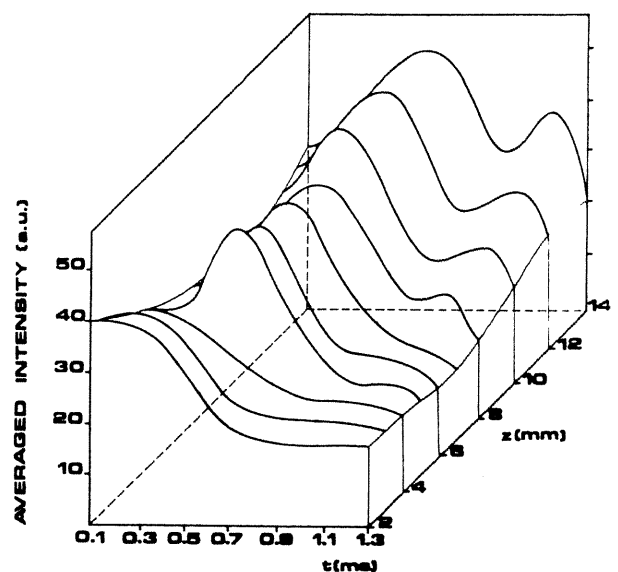


Fig. 4 Temporal profiles of scattering intensities collected on the whole diesel spray cross section for different distances from the nozzle outlet [4].

value nature of the function. This problem can be overcome with integration on narrow scattering angle or wavelength range /1/. Anyway when the collected scattering intensity is relative to a large number of droplets the oscillations are smoothed away. In this case the intensity of scattered light is a measure of surface area of the droplets per unit volume /7/. This kind of measurement can be performed through the sum of the intensity levels of all the pixels in images collected under the conditions of Fig.2c, when the number concentration is very high /4/.

An example of this application is reported in Fig.4 where the temporal profiles of scattering intensities collected on the whole diesel spray cross section are reported for different distances from the nozzle outlet. The relevance of such spatial-temporal behaviour of the total surface area per unit volume (of the droplet cloud in cross sections of diesel spray) and the related experimental conditions are reported in the references /4,8/. In this paper it is sufficient to comment that the oscillation of Fig.4 can be caused by atomization modulations due to not-steady conditions of injections and to two-phase flows generated inside the nozzle prechamber. Similar measurements have been also exploited to show the beneficial influence of the environmental temperature on atomization and the features of the vaporization process for high-pressure injections conditions /9/.

For diluted sprays, like that one of Fig.2b and in the case the scattering intensity dependence on the drop size is a single value function (like the higher line reported in Fig.3, relative to refractive index with high values of the imaginary part) the probability density function of the droplets present in a single image or in an ensemble of images can be obtained. It is computed as the presence frequency of single connected regions with the same intensity level. No results of this kind are reported in the literature.

## TWO-IMAGES SYSTEMS

The possibility of exploiting two scattering patterns for diagnostics purposes relies on the capability of knowing the couple of pixels (one for each image) which corresponds to the same control volume in the real object field. In fact only the possibility of performing mathematical and/or logical operations between different scattering characteristics on the same point make the use of two cameras systems useful.

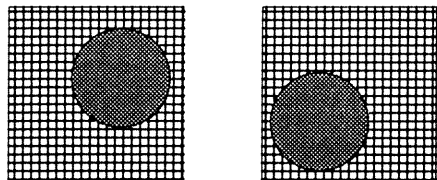


Fig.5 Synthetic image showing as the same object can be imaged in different position of the two detectors. Mechanical and numerical adjustments and pixel grouping techniques can be used to avoid this problem.

This topic is better illustrated by Fig.5. The same object cover different parts of the two cameras. Micrometric mechanical adjustments can be easily performed with a known finite accuracy  $\epsilon_a$ . The two images can be overlapped with an approximation equal to this accuracy  $\epsilon_a$ . In fact, even though  $\epsilon_a$  is smaller than the size of the single pixel, it is possible to align the image contour with the boundary of one pixel; for instance in Fig.5a a small displacement of the camera on the right will "light" the pixel adjacent on the left of the image contour. The same type of alignment can be performed for the image in Fig.5b also in the limit of the accuracy  $\epsilon_a$ .

Similar considerations apply to the procedures needed for obtaining the same magnification ratio on the two cameras.

In order to increase the accuracy of the pixel correspondence a further step is also required. The  $n \times m$  matrix is reduced to  $(n/k) \times (m/k)$  one, summing the intensity levels relative to groups of  $k \times k$  pixels, to form macro pixels. A limit condition is reached when  $k$  is chosen as large as  $m$ . In this case the two matrices of intensities reduce to two values. The same measurement can be performed by means of two single point detectors (e.g. photomultipliers, photodiodes, etc.). But there are some cases where the use of the two cameras is still better. This happens, for instance, in the scattering pattern of diesel spray cross section, since it is a random process for which it is not possible to foresee the size and the position of the droplet cloud. In this case the image becomes a validation criterion of the measure. Furthermore stray light background can also be recognized and neglected by means of spatial filtering.

When that mechanical adjustment cannot be performed with the suitable precision, an alternative procedure, described in the reference /10/, for diluted scatterers fields, can be used. It consists in labelling the "isolated" shapes on the two images, so that a correspondence can be established between scatterers images rather than between single pixels. In Fig.6 a "synthetic" example of two images with different magnification ratios and shifted respect to the image corners indicate an ordered

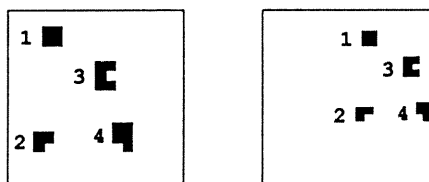


Fig.6 Example of structure recognition in a couple of images detecting the same object set with different magnifications and with a spatial shift.

list of shapes from 1 to 4. For each labelled single-connected image it is possible to compute on the numerical image several characteristics: gravity centers (g.c.), intensity momenta respect to g.c., shape factors. Therefore logical and mathematical operations can be performed on couples of these characteristics without any

care of real size and relative distances of scatterers.

If the alignment between the two images is required and mechanical adjustment systems are not available or mechanical shift (due, for instance, to thermal expansion), occurs, the gravity center coordinates of the scatterers can be numerically shifted in such a way that they are forced to coincide.

All the considerations commented in this section can be used for any couple of images. For instance the two images can be relative to two scattering patterns temporally shifted in order to follow the evolutions of the process or to a

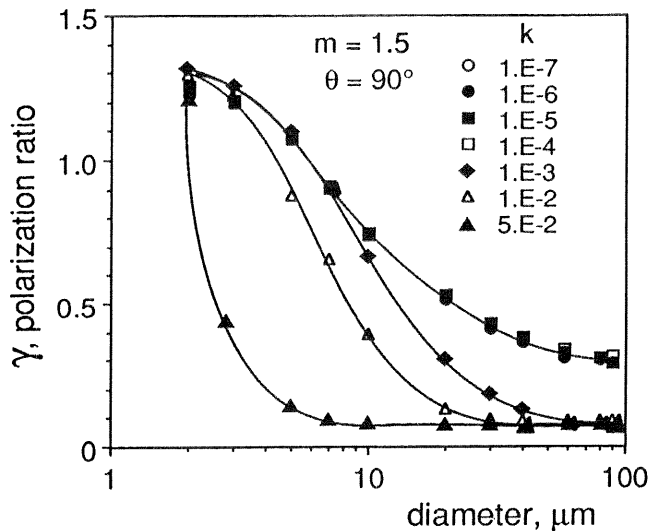


Fig.7  $\gamma$  polarization ratio profiles vs drop diameter calculated for a real part of refractive index of 1.5 and for 7 values of the imaginary part.

couple formed by an elastic light scattering pattern and a fluorescence one or to two patterns with different scattering characteristics. The last operation mode parallels many single point techniques which have been widely exploited in steady process /1/. The most common couple of measurements is related to "horizontally" and "vertically" polarized scattered light linked by their ratio  $\gamma$  (polarization ratio). Details of such techniques are available in references /1,5/, so that only their main features are outlined with the aid of Fig.7, in which they polarization ratios are plotted as drop size function for different imaginary parts of the refractive index. The oscillations described for the vertically polarized cross sections in Fig.3 are smoothed away computing their scattering intensity or small range of sizes and scattering angles, so that a monotonous decreasing function is obtained for all the curves. Higher is the absorptivity of the particle, higher is the steepness of the curve, so that the drop-size range in which the curves are sensible to  $\gamma$  variation, narrows, but for  $k < 10^{-4}$  the dependence on sizes is nearly the same and it can be used for diagnostics purpose. It is worthwhile to stress that, only when the refractive index is known, this plot can be considered calibrations for the drop size. In the burning spray, if liquid pyrolytic processes, which increase

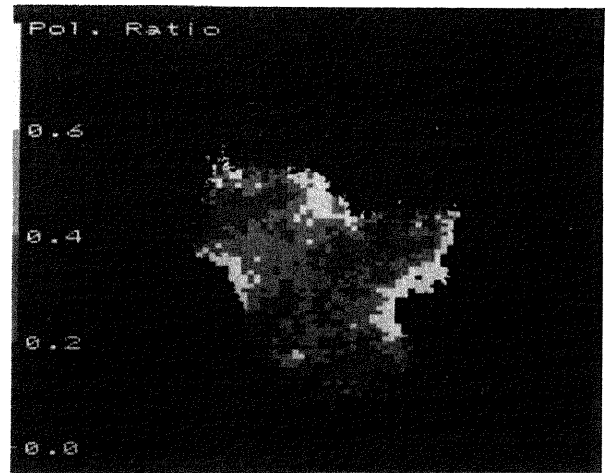


Fig.8 Polarization ratio pattern from a spray cross section at 14 mm from the nozzle in pre-ignition conditions /4/.

the imaginary part of the refractive index, cannot be neglected,  $\gamma$  is only a qualitative descriptor of the scatterers characteristics. High values of  $\gamma$  correspond to large and/or absorbing droplets, which are to be considered in any case unfavourable conditions for the combustion progress. The polarization ratios of submicron-sized scatterers are less sensitive to the size and they are related to only one value when they are much smaller than the illuminating wavelength /5/. Very absorbing particles in this asymptotic limit take  $\gamma$  value lower than 0.08 /12/.

The contemporaneous presence of different kinds of scatterers inside a single control volume related to a single pixel make analysis of  $\gamma$  measurements very difficult to be interpreted. Multiple images at different scattering angles or wavelengths are expected to yield determination of varying refractive index or identification of different scatterers categories, analogously to single-point measurements /1,11/. An example of a polarization ratio pattern is reported in Fig.8 relative to a spray cross section at 14 mm from the nozzle outlet detected 3.1 msec after the needle opening. It is obtained by a couple of images which have been carefully aligned and processed by a code of "grouping", following the procedures mentioned at the beginning of the section.

The black and white printing limits they representation to only four levels, whereas false colour scales can make distinguishable up to ten levels. The scale of  $\gamma$  can also be read in terms of average droplet sizes, since the pattern refers to a diesel spray in pre-ignition conditions and only droplet with the same refractive index are present. The reader is referred to the paper /12/ for further details. Here is only worthwhile to mention that the spatial drop-size distribution, as it can be deduced by Fig.8, is very complex and very small or very large droplets can be randomly present in the periphery of the spray.

Another example of application of the two images scattering systems is reported in Fig.9, in which the pattern of  $\gamma$  lower than 0.08 are



Fig.9 Polarization ratio pattern from a spray cross section at 30 mm from the nozzle in ignition conditions /4/.

reported in a post-ignition condition. These very low  $\gamma$ -values can be attributed only to very small particles in submicron-size range or to large particles with very absorbing optical properties, as it can be deduced by Fig.7. In both cases the  $\gamma$ -values refer to soot particles, i.e. the only particles smaller than microns, or to cenosphere, i.e. liquid pyrolysis product formed by carbonaceous material. The complete discussion /12/ concerning these data yields the conclusion that pyrolysis is "effective" well inside the spray section and consequently the heat release, which generates the pyrolysis and which is linked to oxidative regions, also is distributed inside the spray. This is the first indirect indication that diesel combustion can progress in an "internal combustion mode".

#### FINAL REMARKS

The laser light scattering technique, used for single point measurements in steady state combustion process, can be successfully exploited for two-dimensional characterization of condensed phases in diesel combustion system. Two independent measurements can be simultaneously obtained when two detecting device are synchronized with the illumination pulsed source.

A single measured scattering intensity can be only related to quantities which depend on concentration of the scatterers, whereas the ratio between two intensities is not dependent on concentration and it can be related to physical-chemical characteristics of the scatterers.

In the case of only presence of fuel droplet in the scattering volume quantitative measurements, relative to liquid surface area per unit volume and droplet sizes can be gained; whereas in other conditions only qualitative information can be obtained. In both cases the two-dimensional nature of the technique offers the possibility of analyzing morphological aspects which are relevant in any case also under their qualitative form.

Finally it is of interest to evidence that anelastic effects can be exploited for two-dimensional recognition of gaseous species di-

tribution, and that their combination with the diagnostics presented in this paper are expected to yield the data base for understanding the evolution of combustion processes.

#### REFERENCES

- 1 - Beretta F., Cavaliere A., D'Alessio A.: Proc. of Twentieth Symposium (Int.) on Combustion, p. 1249, The Combustion Institute, 1984,
- 2 - Winter M., Lan J.K., Long M.B.: Exp. in Fluids 5, 177, 1987.
- 3 - Ragucci R., Cavaliere A., Massoli P.: "drop sizing by L.L.S. exploiting Intensity Angular Oscillations in Mie Regime" Particle Characterization, in press.
- 4 - Cavaliere A., Ragucci R., D'Alessio A., Noviello C.: "Analysis of Diesel Sprays through Two-Dimensional Laser Light Scattering", paper presented at the XXII Symposium Int. on Combustion, August 14-19, 1988, USA.
- 5 - D'Alessio A., Beretta F., Cavaliere A., Menna P.: "Soot Combustion System and its Toxic Properties", eds. J Lahaye and G. Prado, p. 237 and p. 335, Plenum Press, N.Y. and London, 1983.
- 6 - Toon O.B., Ackerman T.: Appl. Optics, **20**, 3657, 1981.
- 7 - Glantschnig W.J., Chen S.: Appl. Optics, **20**, 2499, 1981.
- 8 - Cavaliere A., Ragucci R., D'Alessio A., Noviello C.: "Analysis of Dense Sprays Through Two-Dimensional Laser Light Scattering", paper presented at ILASS-EUROPE, Rouen March 28-29, 1989.
- 9 - Cavaliere A., Ragucci R., D'Alessio A., Noviello C., "Atomization and Evaporation of Diesel Sprays in High Pressure and Temperature Environment" submitted for publication on Atomization and Spray, 1990.
- 10 - Ragucci R., Cavaliere A., D'Alessio A., Massoli P.: "Quantitative Measurements from 2D Elastic Scattering Patterns in the Analysis of Two-phase Flows", CMEM 89, Capri May 23-26, 1989, Proc in the volume "Computers and Experiments in Mechanics", G.M. Carlomagno ed., p.189, Napoli, 1989.
- 11 - Beretta F., Cavaliere A., D'Alessio A., Ragucci R.: "Ensemble Laser Light Scattering Technique for the Analysis of Atomization of Coal-water Slurry" Intern. Conf. on Liquid Atomization and Spray Systems - ICLASS 85, London July 8-10, 1985.
- 12 - Cavaliere A., Ragucci R., D'Alessio A., Noviello C., "Digital Imaging of Condensed Phases Fields in Ignited Unsteady Sprays" submitted for publication on Comb. Sci. Techn. 1990.